PHYSICAL REVIEW LETTERS

VOLUME 79 | 13 OCTOBER 1997 | NUMBER 15

Ladder Proof of Nonlocality without Inequalities: Theoretical and Experimental Results

D. Boschi, S. Branca, F. De Martini, and L. Hardy

Dipartimento di Fisica, Istituto Nazionale di Fisica Nucleare, Istituto Nazionale di Fisica della Materia, Università "La Sapienza," Roma 00185, Italy

(Received 27 May 1997)

We show how a previous demonstration of nonlocality without inequalities for two spin-half particles can be improved so that a greater proportion of the pairs are shown to be subject to a contradiction with local realism. This is achieved by considering more settings of the apparatus at each end. Also, we report on an experimental realization employing a tunable source of polarization entangled photons. The experimental results violate locality (modulo, the efficiency loophole). [S0031-9007(97)04135-5]

PACS numbers: 03.65.Bz, 42.50.–p

There have been various demonstrations of nonlocality without inequalities [1–3]. One due to Hardy [3], which can be implemented with two polarization entangled photons (see also [4–6]), has been tested in two experiments [7,8]. However, in this proof, only approximately 9% of the pairs of photons are shown to be subject to a contradiction with local realism. In this paper we show how this percentage can be improved to $(50-\delta)\%$ (where δ is any small finite number). Also we report an experimental demonstration of this effect, employing a tunable source of polarization entangled states (shown in Fig. 1).

We consider a polarization entangled state for two photons of the form

$$|\Psi\rangle = \alpha|+\rangle_A|+\rangle_B - \beta|-\rangle_A|-\rangle_B . \tag{1}$$

On photon A (B) we make polarization measurements along one of the $K+1$ possible directions A_k (B_k), where $k=0$ to K. The corresponding quantum states are $|A_k\rangle$ and $|B_k\rangle$ with orthogonal states $|A_k^\perp\rangle$ and $|B_k^\perp\rangle$, respectively. These states provide an alternative basis for the subsystems A and B, and hence we can write

$$|+\rangle_A = c_k|A_k\rangle + c_k^\perp|A_k^\perp\rangle, \tag{2}$$

$$|-\rangle_A = (c_k^\perp)^*|A_k\rangle - c_k^*|A_k^\perp\rangle, \tag{3}$$

$$|+\rangle_B = c_k|B_k\rangle + c_k^\perp|B_k^\perp\rangle, \tag{4}$$

$$|-\rangle_B = (c_k^\perp)^*|B_k\rangle - c_k^*|B_k^\perp\rangle . \tag{5}$$

In order to have a contradiction between locality and quantum mechanics, we want to choose A_k and B_k such that

$$P_K = \text{Prob}(A_K = 1, B_K = 1) \neq 0 , \tag{6}$$

$$\text{Prob}(A_k = 1, B_{k-1} = 0) = 0 \quad \text{for } k = 1 \text{ to } K , \tag{7}$$

$$\text{Prob}(A_{k-1} = 0, B_k = 1) = 0 \quad \text{for } k = 1 \text{ to } K , \tag{8}$$

$$\text{Prob}(A_0 = 1, B_0 = 1) = 0 . \tag{9}$$

Here, the statement $A_k = 1$ ($A_k = 0$), for example, implies that A_k has been measured and A_k ($A_k^\perp$) is the outcome. First we will show that these properties, in conjunction with locality, lead to a contradiction and then we will show how it is possible to realize them in quantum theory.

Consider the example $K=2$. The "ladder" form of the contradiction is shown in Fig. 2. Assume that, for one particular run of the experiment, A_2 and B_2 have been measured and the results, $A_2 = 1$ and $B_2 = 1$, have been observed [that this is possible follows from prediction (6)]. Assuming local realism, it follows from the result $A_2 = 1$ and prediction (7) that, had B_1 been measured, the result $B_1 = 1$ would have been observed. Similarly, $B_2 = 1$ and (8) imply that, had A_1 been measured, the result $A_1 = 1$ would have been observed. This takes us one rung down the ladder (Fig. 2). We can repeat this to go down again, obtaining $A_0 = 1$ and $B_0 = 1$. Hence, it follows from local realism that $A_0 = 1$ and $B_0 = 1$ with probability at least equal to P_K, which contradicts

 © 1997 The American Physical Society

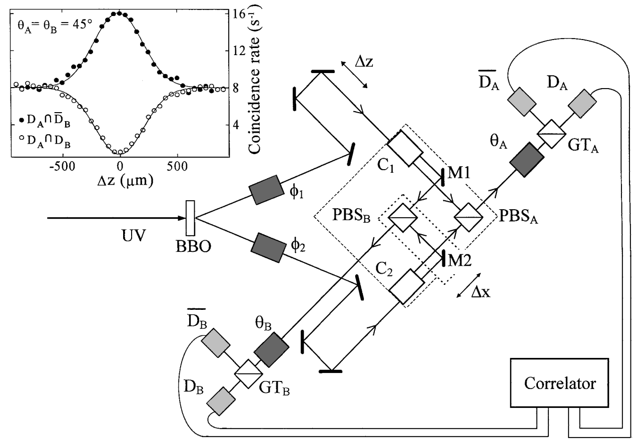

FIG. 1. The experimental arrangement. The dotted lines show the invar table and slide used to vary Δx. The inset shows a typical scan over Δz showing visibility of about 92%.

prediction (9). Similar reasoning applies for other values of K. Hence, local realism is incompatible with the above properties. The special case, where $K = 1$, was given in [3]. It has been pointed out by Stapp [4] that the $K = 1$ case is equivalent to a logical contradiction of the form $A \Rightarrow B \Rightarrow C \Rightarrow D$, but $A \nRightarrow D$. The general case is then equivalent to a contradiction of the form $A \Rightarrow B \Rightarrow \cdots \Rightarrow Z$, but $A \nRightarrow Z$.

We will now show how properties (6)–(9) can be realized in quantum theory. For simplicity, we will take α and β to be real and positive, and we will take c_k and $c_k^\perp$ to be real (corresponding to linear polarizations). Property (9) requires

$$(\langle A_0| \langle B_0|) |\Psi\rangle = 0 . \tag{10}$$

Using (1)–(5), this gives $\alpha c_0^2 - \beta (c_0^\perp)^2 = 0$ which is satisfied when

$$c_0 = N\beta^{1/2}, \qquad c_0^\perp = N\alpha^{1/2}, \tag{11}$$

where N is a real constant. Property (7) requires

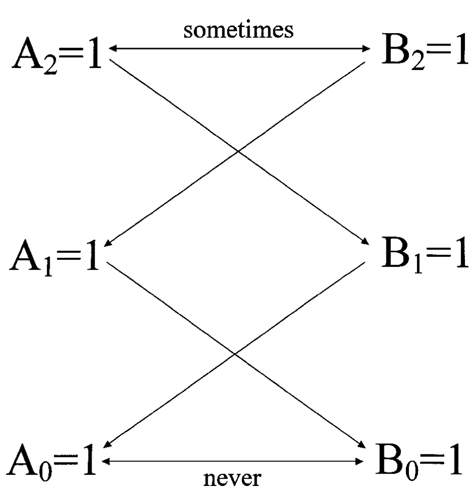

FIG. 2. The form of the ladder contradiction for case $K = 2$.

$$(\langle A_k| \langle B_{k-1}^\perp|) |\Psi\rangle = 0 , \tag{12}$$

and property (8) requires

$$(\langle A_{k-1}^\perp| \langle B_k|) |\Psi\rangle = 0 . \tag{13}$$

Both of the above equations lead to $\alpha c_k c_{k-1}^\perp + \beta c_k^\perp c_{k-1} = 0$. To satisfy this, we can write

$$c_k = -N'\beta c_{k-1} , \qquad c_k^\perp = N'\alpha c_{k-1}^\perp , \tag{14}$$

where N' is a real constant. From Eqs. (11) and (14), we obtain

$$c_k = N''(-1)^k \beta^{k+1/2}, \qquad c_k^\perp = N''\alpha^{k+1/2}, \tag{15}$$

where N'' is a real constant. The probability P_K is given by

$$P_K = |(\langle A_K| \langle B_K|) |\psi\rangle|^2. \tag{16}$$

Using (1)–(5), we obtain

$$P_K = |\alpha c_K^2 - \beta (c_K^\perp)^2|^2. \tag{17}$$

Substituting Eq. (15) into this, and remembering normalization, we obtain

$$P_K = \left(\frac{\alpha\beta^{2K+1} - \beta\alpha^{2K+1}}{\beta^{2K+1} + \alpha^{2K+1}} \right)^2 . \tag{18}$$

If we have a maximally entangled state so that $\alpha = \beta$ initially, then $P_K = 0$ for all K, and there is no contradiction with local realism. If we choose $K = 1$, then it can be shown that the maximum value of P_1 is 9.0% realized when $\alpha/\beta = 0.46$. This is the case previously considered in [3]. If we take $K = 2$, then we find that the maximum value of P_2 is 17.5% realized when $\alpha/\beta = 0.57$. When $K = 3$, the maximum value of P_3 is 23.5% realized when $\alpha/\beta = 0.64$. As we increase K we also increase the maximum value of P_K, and the value of α/β required to realize the maximum tends towards the value 1 (the value taken for a maximally entangled state). From (18) we see that, as $K \to \infty$, $P_K \to \min(\alpha^2, \beta^2)$ for $\alpha \neq \beta$. Since $a = \beta = 1/\sqrt{2}$ gives $P_K = 0$, we see that the maximum value of P_K is (50$-\delta$)% and is realized for large K and a state that is not quite maximally entangled.

In a real experiment, inequalities are necessary to show that the errors do not wash out the logical contradiction that local realism faces. The Clauser-Horne inequalities can be written [6]

$$\begin{aligned} &\mathrm{Prob}(A_k = 1, B_k = 1) - \mathrm{Prob}(A_{k-1} = 1, B_{k-1} = 1) \\ &\quad \leq \mathrm{Prob}(A_k = 1, B_{k-1} = 0) + \mathrm{Prob}(A_{k-1} = 0, B_k = 1) . \end{aligned} \tag{19}$$

Using a method similar to that of Braunstein and Caves [9], we sum these inequalities over $k = 1$ to K and we get

$$\mathrm{Prob}(A_K = 1, B_K = 1) - \mathrm{Prob}(A_0 = 1, B_0 = 1) \leq \sum_{k=1}^{K} [\mathrm{Prob}(A_k = 1, B_{k-1} = 0) + \mathrm{Prob}(A_{k-1} = 0, B_k = 1)]. \quad (20)$$

Since all term, except the first in this inequality, are equal to zero in the ideal case, the inequality is violated by an amount equal to P_K [given in Eq. (18)]. In fact, following the method in [10], the inequality (20) can be derived by expressing the probabilistic condition that the above contradiction should never happen.

Now we will describe the actual experiment, as shown in Fig. 1. A BBO (β-barium borate) crystal cut for type-I phase matching (optical axis is at 33°) is pumped by a 200 mW UV cw argon laser (with wavelength 351.1 nm). Pairs of photons with the same wavelength (702.2 nm) are selected by diaphragms in paths 1 and 2 (as shown in Fig. 1). These photons initially have horizontal (or ordinary) polarization so that the initial state is $|o\rangle_1|o\rangle_2$. Next the photons pass through Fresnel rhomb polarization rotators with variable angle settings ϕ_1 and ϕ_2, and the state becomes

$$[\cos(\phi_1)\,|o\rangle_1 + \sin(\phi_1)\,|e\rangle_1][\cos(\phi_2)\,|o\rangle_2 + \sin(\phi_2)\,|e\rangle_2]. \quad (21)$$

Here e represents vertical (extraordinary) polarization. Path 1 passes through a trombone arrangement (with displacement parameter Δz) which is used to overlap the photon wave packets to get the correct conditions for interference. This displacement is varied by a computer controlled micrometrical stage. After this each photon passes through a 4 cm long calcite crystal splitting the ordinary and extraordinary polarizations onto separate paths. The extraordinary path $1'$ from calcite crystal 1 impinges on one input port of polarizing beam splitter A, and the ordinary path 2 from calcite crystal 2 impinges on the other input port of this polarizing beam splitter. Similarly, the ordinary path 1 from calcite crystal 1 and the extraordinary path $2'$ from calcite crystal 2 impinge on the two input paths of polarizing beam splitter B. If the total path lengths to the polarizing beam splitters (measured, say, from the BBO crystal) are denoted by $x_{1,2}^{o,e}$ (in an obvious notation) then the state just before these beam splitters is

$$[\cos(\phi_1)e^{ix_1^o}\,|o\rangle_1 + \sin(\phi_1)e^{ix_1^e}\,|e\rangle_{1'}] \times [\cos(\phi_2)e^{ix_2^o}\,|o\rangle_2 + \sin(\phi_2)e^{ix_2^e}\,|e\rangle_{2'}]. \quad (22)$$

The polarizing beam splitters (which here are actually functioning as "beam mergers") are oriented so that they transmit ordinary polarization and reflect extraordinary polarization. Hence, all photons end up in paths A and/or B, and the state becomes

$$[\cos(\phi_1)e^{ix_1^o}\,|o\rangle_B + i\sin(\phi_1)e^{ix_1^e}\,|e\rangle_A] \times [\cos(\phi_2)e^{ix_2^o}\,|o\rangle_A + i\sin(\phi_2)e^{ix_2^e}\,|e\rangle_B] \quad (23)$$

(where the phase factor i is picked up on reflection). We postselect only those cases where one photon goes to each end so that the effective state becomes

$$\cos(\phi_1)\cos(\phi_2)e^{i(x_1^o+x_2^o)}\,|o\rangle_A|o\rangle_B - \sin(\phi_1)\sin(\phi_2)e^{i(x_1^e+x_2^e)}\,|e\rangle_A|e\rangle_B. \quad (24)$$

Finally, paths A and B are analyzed in linear polarization at an angle $\theta_{A,B}$ by means of a polarization rotator $\theta_{A,B}$ and a fixed Glan-Taylor polarizing beam splitter oriented to transmit ordinary (horizontal) and reflect extraordinary polarization. Detectors $D_A(\theta_A)$ (in the transmitted path) and $\overline{D}_A(\theta_A)$ (in the reflected path) are on the A side, and similarly $D_B(\theta_B)$ and $\overline{D}_B(\theta_B)$ are on the B side. The detectors were equal cooled avalanche Si diodes (EGG-SPCM-200PQ) with quantum efficiency equal to about 60% and a noise rate of about 100 Hz. Before each detector is a diaphragm and a 0.4 nm interferential filter which defines a coherence length of 500 μm [11]. These very narrow filters were used to reduce the effects of dispersive elements in the setup. If $e^{i(x_1^o+x_2^o)} = e^{i(x_1^e+x_2^e)}$, Eq. (24) is of the same form as Eq. (1). To arrange this condition, a "trombone" was formed by mounting mirror $M2$ and polarizing beam splitter B on a slide that can be moved in a direction parallel to path B through a displacement Δx (this displacement was computer controlled via a piezoelectric mounting). In order to ensure greater stability against temperature fluctuations, this slide was constructed from the alloy invar (which has a very low expansion coefficient) and, furthermore, the slide, the mirror $M1$, and the polarizing beam splitter A were all mounted on a small table also constructed from invar. Δz was set to ensure the correct time conditions for interference (the cases where both photons go the same way were useful in accomplishing this), then Δx was set to ensure the correct phase of entanglement. The visibility measured when Δz was varied was about 92% (Fig. 1).

For a given value of K the optimum value of α/β which maximizes P_K [calculated from Eq. (18)] is realized by appropriate settings of ϕ_1 and ϕ_2. We can write

$$|A(\theta)\rangle = \cos(\theta_A)\,|+\rangle_A + \sin(\theta_A)\,|-\rangle_A,$$

where $(+)$ corresponds to o and $(-)$ corresponds to e. By taking the inverse of Eqs. (2) and (3) and using (15), we find that the appropriate setting of θ_A for measuring A_k (and similarly for B_k) is given by

$$\tan(\theta_A^k) = \tan(\theta_B^k) = (-1)^k(\alpha/\beta)^{k+1/2}. \quad (25)$$

Once K has been chosen and $\Delta z, \Delta x, \phi_1$, and ϕ_2 are set appropriately, the count rates corresponding to the joint probabilities appearing in Eqs. (6)–(9) can be measured by using the transmitted channels in each case. The count time for each measurement was 300 s. The need to stabilize phase variations meant that longer count times could not be used. To obtain probabilities these rates

K=1

$(\theta_A, \theta_B)(^\circ)$	$P(\theta_A, \theta_B)$
$(\theta_1 = -18, \theta_1 = -18)$	0.089 ± 0.008
$(\theta_1 = -18, \theta_0^\perp = +34^\perp)$	0.008 ± 0.002
$(\theta_0^\perp = +34^\perp, \theta_1 = -18)$	0.009 ± 0.002
$(\theta_0 = +34, \theta_0 = +34)$	0.013 ± 0.003

K=2

$(\theta_A, \theta_B)(^\circ)$	$P(\theta_A, \theta_B)$
$(\theta_2 = +14, \theta_2 = +14)$	0.17 ± 0.01
$(\theta_2 = +14, \theta_1^\perp = -23^\perp)$	0.007 ± 0.002
$(\theta_1^\perp = -23^\perp, \theta_2 = +14)$	0.013 ± 0.003
$(\theta_1 = -23, \theta_0^\perp = +37^\perp)$	0.020 ± 0.004
$(\theta_0^\perp = +37^\perp, \theta_1 = -23)$	0.014 ± 0.003
$(\theta_0 = +37, \theta_0 = +37)$	0.029 ± 0.006

K=3

$(\theta_A, \theta_B)(^\circ)$	$P(\theta_A, \theta_B)$
$(\theta_3 = -12, \theta_3 = -12)$	0.23 ± 0.04
$(\theta_3 = -12, \theta_2^\perp = +18^\perp)$	0.010 ± 0.002
$(\theta_2^\perp = +18^\perp, \theta_3 = -12)$	0.019 ± 0.006
$(\theta_1^\perp = -27^\perp, \theta_2 = +18)$	0.029 ± 0.007
$(\theta_2 = +18, \theta_1^\perp = -27^\perp)$	0.024 ± 0.006
$(\theta_1 = -27, \theta_0^\perp = +38.5^\perp)$	0.025 ± 0.007
$(\theta_0^\perp = +38.5^\perp, \theta_1 = -27)$	0.041 ± 0.009
$(\theta_0 = +38.5, \theta_0 = +38.5)$	0.033 ± 0.008

K	N_C	S
1	5595 ± 130	0.059 ± 0.008
2	13620 ± 240	0.09 ± 0.01
3	3540 ± 178	0.05 ± 0.03

FIG. 3. Tables of the experimental results for the cases $K = 1, 2, 3$.

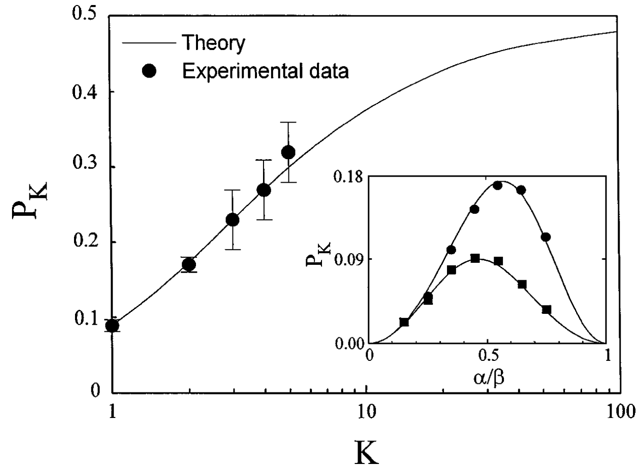

FIG. 4. Plot of P_K against K. The inset shows plots of P_1 (■) and P_2 (●) against α/β. The solid curves are the theoretical predictions.

were normalized by dividing N_c, which is given by four times the count rate measured when $\phi_1 = \phi_2 = \theta_A = \theta_B = 45^\circ$ and Δz was far from the value required for interference (see the inset in Fig. 1). Measurements were made for $K = 1, 2, 3$, and the results are shown in Fig. 3. In each case, the probability corresponding to P_K is very different from zero and the remaining probabilities are close to zero. This is as close as one can reasonably expect to get to an experimental verification of nonlocality without inequalities. To be sure that there is a violation of local realism we can see that the inequalities (20) are violated by the amount S, shown in Fig. 3, in each case.

The count rate corresponding to P_K was measured for the cases $K = 1, 2, 3, 4, 5$. The results are shown in Fig. 4. (Note that for the cases $K = 4, 5$ other count rates were not measured, and that the angles used were calculated theoretically as explained above.) The convergence to 50% is very slow.

All the experimental results mentioned so far correspond to the case where α and β are chosen to maximize P_K. Additional measurements of P_K were made for a range of values of α/β for $K = 1, 2$. The angle θ_K is calculated in each case using Eq. (25). These results are plotted in the inset of Fig. 4.

In this paper it has been shown how it is possible to obtain a contradiction between quantum mechanics and local realism without inequalities for almost 50% of pairs. Furthermore, an experiment employing a tunable source of polarization entangled photons has been performed to test the relevant predictions of quantum theory.

We would like to thank Giovanni Di Giuseppe for a number of important discussions, and the CEE-TMR (Contract No. ERBFMRXCT96-0066) and INFM (Contract No. PRA97-cat) for funding.

[1] P. Heywood and M. L. G. Redhead, Found. Phys. **13**, 481 (1983).
[2] D. M. Greenberger, M. A. Horne, and A. Zeilinger, in *Bell's Theorem, Quantum Theory and Conceptions of the Universe,* edited by M. Kafatos (Kluwer, Dordrecht, 1989).
[3] L. Hardy, Phys. Rev. Lett. **71**, 1665 (1993).
[4] H. P. Stapp, *Mind, Matter, and Quantum Mechanics* (Springer-Verlag, Berlin, 1993); Am. J. Phys. **65**, 300 (1997).
[5] S. Goldstein, Phys. Rev. Lett. **72**, 1951 (1994).
[6] N. D. Mermin, Am. J. Phys. **62**, 880 (1995).
[7] J. R. Torgerson, D. Branning, C. H. Monken, and L. Mandel, Phys. Lett. A **204**, 323 (1995).
[8] G. Di Giuseppe, F. De Martini, and D. Boschi, Phys. Rev. A **56**, 176 (1997); Phys. Lett. A **228**, 208 (1997).
[9] S. L. Braunstein and C. M. Caves, Ann. Phys. (N.Y.) **202**, 22 (1990).
[10] L. Hardy, Phys. Lett. A **161**, 21 (1991).
[11] This experiment does not solve the detection efficiency loophole. We have to assume that the detectors sample the ensemble in a fair way.